crystals

MDPI

Article

Synthesis, Crystal Structure, and Luminescent Properties of New Zinc(II) and Cadmium(II) Metal-Organic Frameworks Based on Flexible Bis(imidazol-1-yl)alkane Ligands

Marina Barsukova [1], Tatiana Goncharova [2], Denis Samsonenko [1,3], Danil Dybtsev [1,3] and Andrei Potapov [2,4,*]

[1] Nikolaev Institute of Inorganic Chemistry, Siberian Branch of the Russian Academy of Sciences, Lavrentieva Ave. 3, 630090 Novosibirsk, Russia; barsukova@niic.nsc.ru (M.B.); denis@niic.nsc.ru (D.S.); dan@niic.nsc.ru (D.D.)

[2] Department of Chemical Engineering, Altai State Technical University, 46 Lenin Ave., 656038 Barnaul, Russia; lira650810@mail.ru

[3] Department of Natural Sciences, Novosibirsk State University, Pirogova Str. 2, 630090 Novosibirsk, Russia

[4] Department of Biotechnology and Organic Chemistry, National Research Tomsk Polytechnic University, 30 Lenin Ave., 634050 Tomsk, Russia

* Correspondence: potapov@tpu.ru; Tel.: +7-923-403-4103

Academic Editors: Claudia Rawn and Winnie Wong-Ng
Received: 1 September 2016; Accepted: 11 October 2016; Published: 13 October 2016

Abstract: New metal-organic frameworks (MOFs) based on zinc and cadmium ions, terephthalic acid, and flexible ligands 1,5-bis(imidazol-1-yl)pentane or 1,6-bis(imidazol-1-yl)hexane were prepared and characterized by X-ray diffraction, thermorgavimetric analysis and IR spectroscopy. The imidazolyl ligands were prepared by a new robust procedure involving the reaction between imidazole and 1,5-dibromopentane or 1,6-dibromohexane in a superbasic medium (KOH in DMSO). MOFs based on 1,5-bis(imidazol-1-yl)pentane had diamond topology (**dia**) and are triply interpenetrated. Ligands with longer spacer 1,6-bis(imidazol-1-yl)hexane, terephthalate ions and zinc(II) ions formed five-fold interpenetrated metal-organic framework also with **dia** topology, while cadmium(II) ions with the same ligands formed eight-connected uninodal net with a very rare self-penetrated topological type **ilc** and a point symbol $4^{24}.5.6^3$. The influence of the chemical composition of MOFs on their photoluminescent properties is investigated and discussed in detail.

Keywords: imidazole; bis(imidazol-1-yl)alkanes; zinc; cadmium; metal-organic frameworks; luminescence; flexible ligands

1. Introduction

Ongoing research aimed at the design of new metal-organic frameworks (MOFs) is stimulated by their high capacity for gas storage and separation [1–6] photo-physical properties [7–10], sensor capabilities [11], excellent catalytic activity [12,13], medical imaging and drug delivery applications [14,15]. Functional properties of MOFs can be fine-tuned by careful choice of organic linkers, both rigid and flexible ligands are suitable for this aim [16]. The use of flexible ligands often hinders the formation of ordered 3D MOF structure, but on the other hand, conformationally mobile molecules can meet the geometrical demands of different metal coordination spheres and form structures otherwise inaccessible with rigid ligands [17]. Poly(azole)-based ligands have been widely used for the construction of MOFs, but most of them act as anionic azolate linkers [18], while neutral bidentate ligands are less explored. Among these ligands, bis(azol-1-yl)alkanes

ligands have been mostly used as chelating ligands to prepare molecular complexes or linear coordination polymers [19,20]. Recently, several papers reporting the use of bis(imidazol-1-yl) or bis(1,2,4-triazol-1-yl) derivatives for building of coordination polymers with extended networks appeared [21–32]. In this contribution we report the synthesis of four new MOFs based on zinc(II) or cadmium(II) ions, terephthalic acid (H_2bdc), and flexible ligands with longer polymethylene linkers, namely 1,5-bis(imidazol-1-yl)pentane (**C5**) or 1,6-bis(imidazol-1-yl)hexane (**C6**), synthesized by an improved procedure, which is also described here. The solid-state luminescence measurements of the title coordination polymers reveal the major influence of the length of the flexible bis(imidazolyl) linkers on the optical properties of the compounds.

2. Results and Discussion

2.1. Synthesis of the Ligands

Although the preparation of **C5** and **C6** ligands was reported by several groups before, their syntheses involved the use of metal potassium [33], sodium imidazolates [34,35], some procedures required inert atmosphere [36–38]. Based on our previous successful preparation of pyrazole derivatives in a superbasic medium KOH-DMSO [39,40], we have developed a new procedure for the synthesis of bis(imidazol-1-yl)alkanes, that does not require toxic solvents, hazardous alkali metals, or special experimental techniques and yields the ligands on a multigram scale (Scheme 1). The reaction between imidazole and corresponding dibromoalkanes proceeded smoothly to give ligands C5 and C6 in high yields.

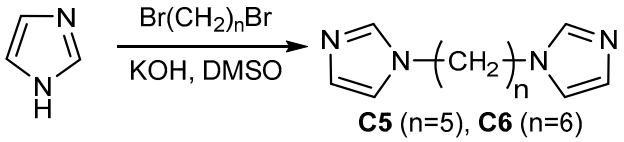

Scheme 1. Synthesis of the ligands in a superbasic medium.

*2.2. Synthesis of Coordination Polymers **1**–**4***

The single crystals of the coordination polymers were obtained by heating solutions containing equimolar amounts of zinc or cadmium nitrates and terephthalic acid and a slight excess (10%) of bis(imidazole) ligand **C5** or **C6**. The solvent composition was optimized in each case to achieve the highest yields and best crystallinity of phase pure products, thus, the mixture of DMF and methanol (1:1) was used as solvent except for compound **1**, for which pure DMF was used. The crystal structures of the title compounds were established by a single crystal X-ray diffraction method. Phase purity of the precipitates obtained was confirmed by comparison of experimental XRD data and patterns calculated from the crystal structure (see below). The XRD plots for compounds **1**–**4** are shown in Figures S1–S4 (supplementary materials). Also, all products were characterized by infrared spectroscopy, elemental analysis, and thermogravimetric analysis.

According to the elemental analysis data coordination polymers **1**, **2**, and **4** contain lattice solvent molecules, their presence was also confirmed by X-ray diffraction analysis. The quantity of the solvent is in accordance with TGA results. The initial weight loss for compounds **1**, **2**, and **4** occurs in the range 80–200 °C; desolvated polymers are stable up to about 350 °C and decompose rapidly at higher temperatures. The TG plots are shown in Figures S5–S8 (supplementary materials).

*2.3. Crystal Structures of Compounds **1**–**4***

The compounds **1** and **2** were found to be isostructural. The asymmetric unit of the compound **1** contains Zn(II) cation, bdc^{2-} anion, **C5** ligand, and one DMF molecule. Zinc cation has a distorted tetrahedral coordination environment built by two N atoms of two **C5** ligands and two O atoms of

two bdc^{2-} anions (Figure 1). Zn–N bond lengths are 1.9987(15) and 2.0273(16) Å. Zn–O bond lengths are 1.9581(14) and 1.9714(12) Å. Carboxylate groups of bdc^{2-} anions are coordinated to Zn(II) cation in a monodentate manner. An uncoordinated carboxylate oxygen atom of one of bdc^{2-} anions is disordered over two positions with s.o.f. 0.412(16)/0.588(16) (Figure 1). Zinc cations are interconnected via bridging bdc^{2-} and C5 ligands to form a metal-organic framework (Figure 2) with a diamond topology (**dia**) while the overall crystal structure of both **1** and **2** results from a triple interpenetration of such nets (Figure 3). Despite the interpenetration, a moderate guest-accessible volume was found (25.2% according to PLATON calculations [41]), apparently occupied by guest DMF molecules.

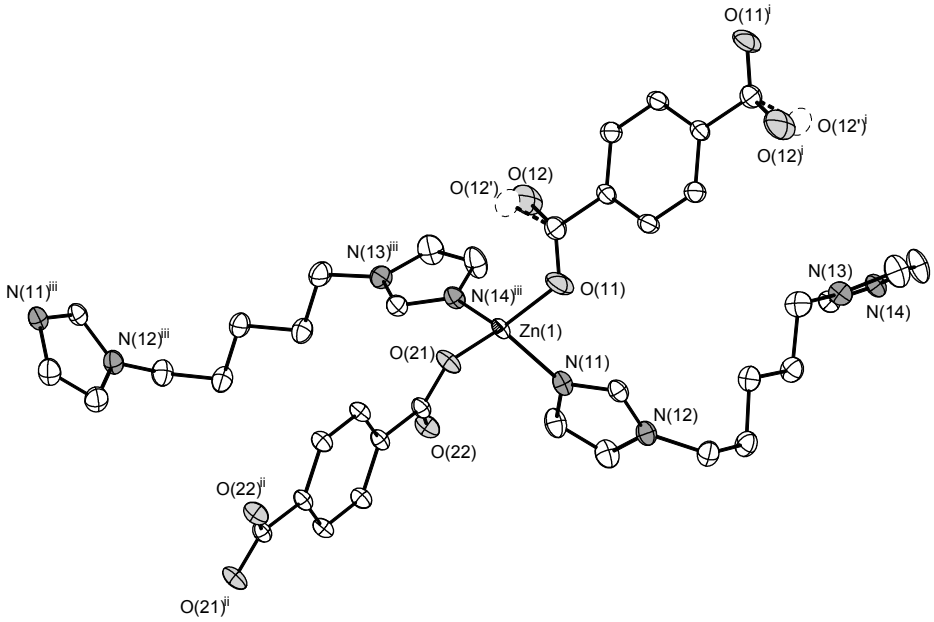

Figure 1. Coordination environment of Zn(II) cation in **1** (ellipsoids of 50% probability). Hydrogen atoms are omitted. Symmetry transformations used to generate equivalent atoms: (i) $1-x, -y, 1-z$; (ii) $-x, -y, -1-z$; (iii) $-1+x, \frac{1}{2}-y, -\frac{1}{2}+z$.

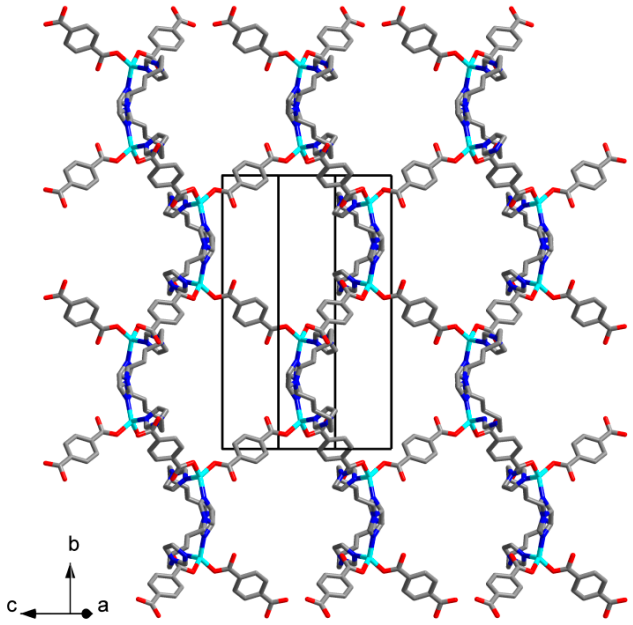

Figure 2. The projection of the single metal-organic framework in **1** along *ac* plane. Hydrogen atoms are omitted.

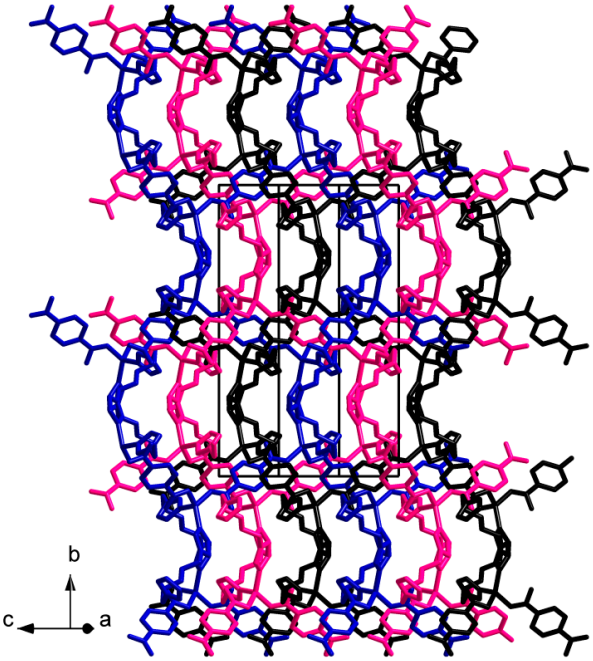

Figure 3. Crystal packing in **1.** Three independent **dia** subnets are highlighted by different colors. Guest DMF molecules and hydrogen atoms are omitted.

The compound **2** features almost the same structure with a slight difference in a local coordination environment of Cd(II) cation. Cd(II) cation also coordinates four ligands (2 bdc^{2-} and 2 C5) playing a role of the four-connecting tetrahedral node. The difference is bidentate coordination of carboxylate groups of bdc^{2-} anions (Figure 4) because of larger ionic radius of Cd(II) cation. Cd–N bond lengths are 2.2355(14) and 2.2561(15) Å. Cd–O bond lengths are in range 2.2782(12)–2.4848(13) Å (average 2.37(9) Å). The void volume occupied by guest DMF molecules is 24.8% according to PLATON estimations, similar to that in **1**.

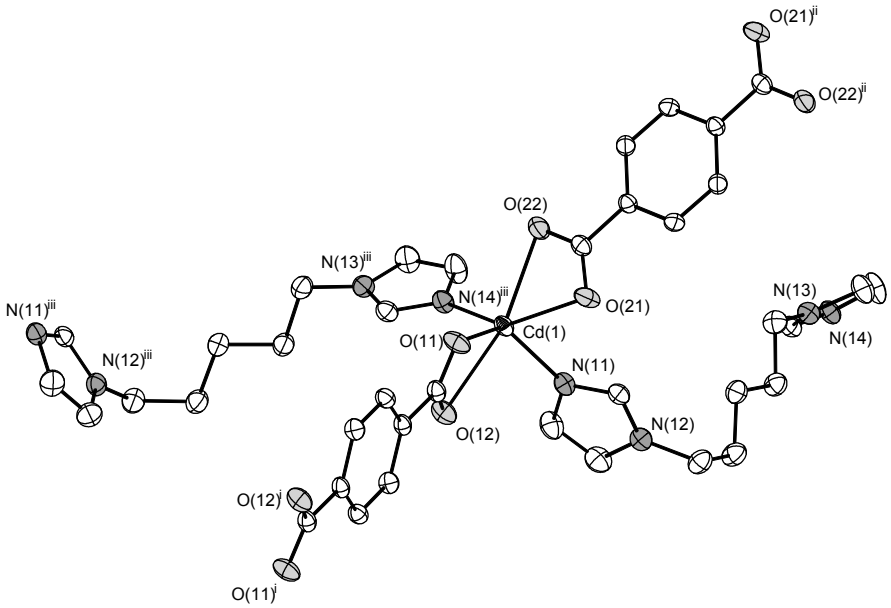

Figure 4. Coordination environment of Cd(II) cation in **2** (ellipsoids of 50% probability). Hydrogen atoms are omitted. Symmetry transformations used to generate equivalent atoms: (i) $-x, -y, -z$; (ii) $1-x, -y, 2-z$; (iii) $-1+x, \frac{1}{2}-y, -\frac{1}{2}+z$.

The asymmetric unit of the structure **3** contains three Zn(II) cations, three bdc^{2-} anions, and three C6 ligands. All Zn(II) cations have similar tetrahedral coordination environment built by two N atoms of two C6 ligands and two O atoms of two bdc^{2-} anions coordinating in a monodentate manner (Figure 5). Zn–O bond lengths are in range 1.98(2)–2.05(3) Å. Zn–O bond lengths are in range 1.94(3)–2.12(3) Å. Zn(II) cations are interconnected via bridging bdc^{2-} and C6 ligands to form a five-fold interpenetrated metal-organic framework (Figure 6) with diamond-like topology **dia**. This results in a rather dense structure containing no residual solvent accessible voids.

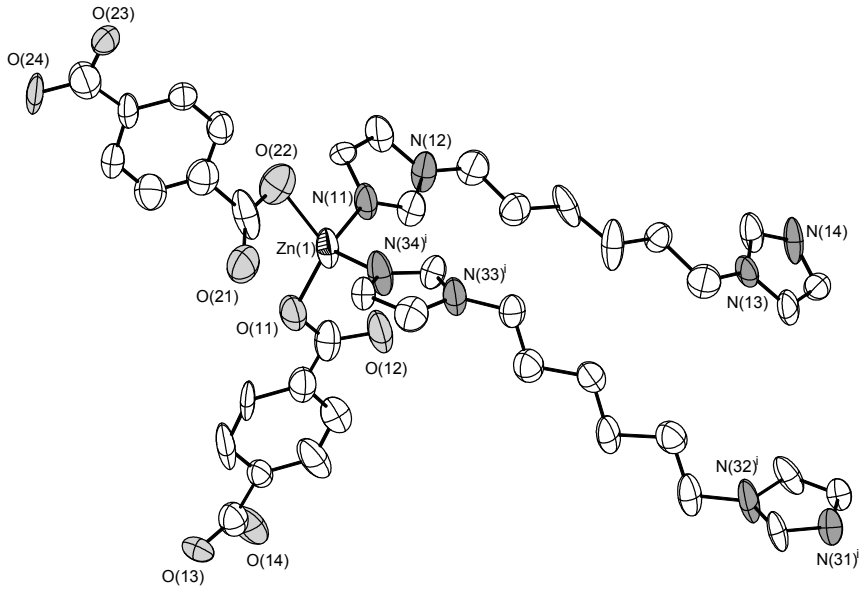

Figure 5. Coordination environment of Zn(II) cation in **3** (ellipsoids of 50% probability). Hydrogen atoms are omitted. Symmetry transformations used to generate equivalent atoms: (i) 1 + *x*, *y*, *z*.

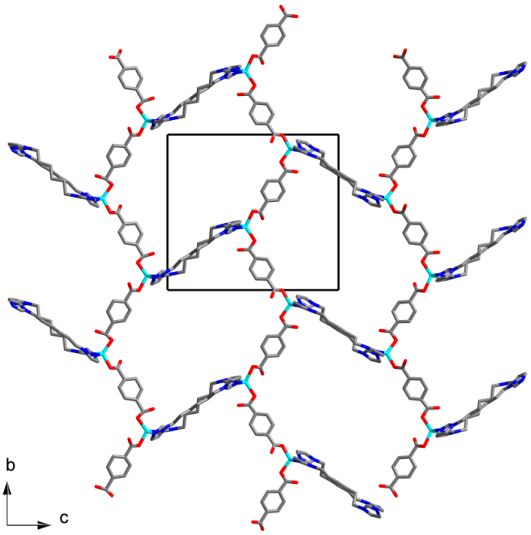

Figure 6. Structure of metal-organic framework in **3**. Hydrogen atoms are omitted.

The asymmetric unit of the structure **4** consists of a Cd(II) cation, a bdc^{2-} anion, a C6 ligand and a methanol molecule. The Cd(II) cation coordinates four carboxylate O atoms of three bdc^{2-} anions and two N atoms of two C6 ligands (Figure 7). The coordination environment of a Cd(II) cation can be described as distorted trigonal bipyramid where one of equatorial positions is occupied by bidentate carboxylate group of bdc^{2-} anion. Cd–N bond lengths are 2.259(3) and 2.324(4) Å. Cd–O bond lengths

lie in range 2.216(3)–2.446(3) Å (average 2.34(10) Å). Two Cd(II) cations are interconnected via two bridging carboxylate groups to form binuclear $\{Cd_2(\mu_2\text{-}OOCR)_2(OOCR)_2(C6)_4\}$ secondary building unit (SBU, Figure 8). Each SBU is joined with eight other SBUs via four bridging bdc^{2-} anions and four bridging **C6** ligands to form 8-c uninodal net with a very rare self-penetrated topological type **ilc** and a point symbol $4^{24}.5.6^3$ [42,43]. The crystal packing in **4** is shown on Figure 9. The void volume occupied by guest methanol molecules was calculated to be 14.8% according to PLATON routine.

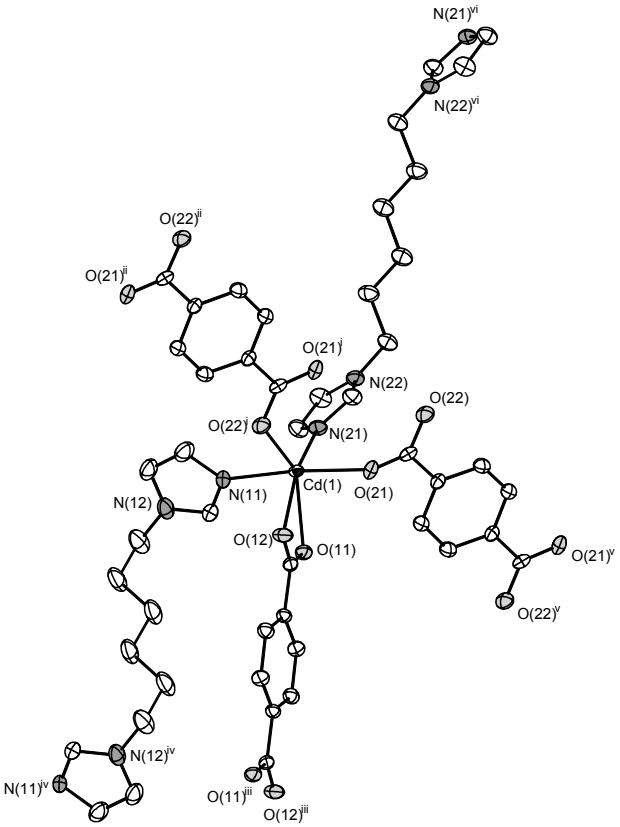

Figure 7. Coordination environment of Cd(II) cation in **4** (ellipsoids of 50% probability). Hydrogen atoms are omitted. Symmetry transformations used to generate equivalent atoms: (i) $2-x, 1-y, -z$; (ii) $x, 1+y, z$; (iii) $2-x, 1-y, 1-z$; (iv) $1-x, 1-y, 1-z$; (v) $2-x, -y, -z$; (vi) $1-x, -y, -1-z$.

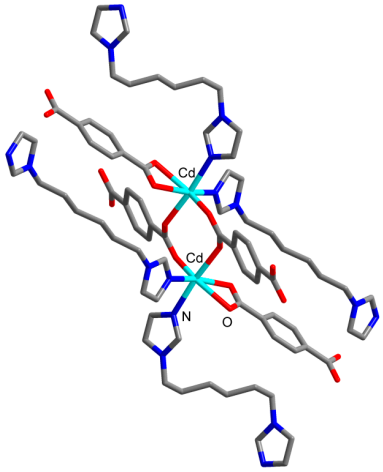

Figure 8. Structure of binuclear $\{Cd_2(\mu_2\text{-}OOCR)_2(OOCR)_2(C6)_4\}$ secondary building unit in **4**. Hydrogen atoms are omitted.

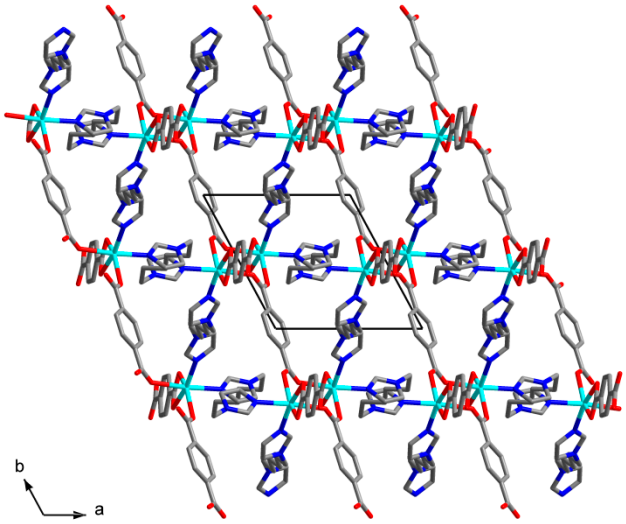

Figure 9. Crystal packing in **4**. Hydrogen atoms are omitted.

The analysis of the chemical compositions and crystal structures of the title compounds could lead to a number of both expected and unexpected conclusions. First of all, the chemical formulas for **1**–**4** comprise an equimolar ratio of metal and organic ligands, the same as for the starting reaction mixtures. The ratio of one metal cation to two bidentate ligands often facilitates a four-connected network of coordination compounds and this is exactly the case for **1**–**3**. Both Zn(II) and Cd(II) metals possess the d^{10} electronic configuration and hence no particular coordination geometry is stabilized by a crystal field. Bearing in mind such flexibility of the coordination environment of the metal cations as well as the bisimidazolyl ligands, the formation of diamond-like net (**dia**) in **1**–**3** is, therefore, not unexpected as this is the overwhelmingly common topology type for four-connected 3D networks. Surprisingly enough, the compound **4** is based on the completely different eight-connected nodes assembled into a very rare **ilc** topology. To the best of our knowledge, this compound is only the third case where such topology was identified [42,43]. Since the reaction conditions for the crystals growth of the title compounds were virtually the same, it is not clear what could be the driving force for the formation of such unique network in **4**. Nevertheless, relatively high yield and chemical purity suggest that this is likely a thermodynamically stable product rather than a metastable kinetically hindered intermediate. It is worth mentioning that the degree of interpenetration of the **dia** net in isoreticular frameworks **1**–**3** correlates with the length of the bridging ligands. Indeed, the shorter C5 ligand in **1** and **2** allows three-fold interpenetration while a somewhat longer C6 affords structure **3** five-fold interpenetration.

2.4. Luminescence Properties

Cadmium(II) and zinc(II) coordination complexes are well known to demonstrate interesting luminescent properties [44–47], which prompted us to investigate the photoluminescence of title compounds. The powder samples were measured at under as similar conditions as possible (freshly prepared compounds, same procedure of pellet formation, measurements during the same day, etc.) to minimize errors during the direct comparison of the results. The excitation and emission spectra are shown on Figure 10. Emission luminescence spectra with normalized intensities are shown on Figure S13 (supplementary materials). The emission spectra are composed of two major independent components, which could be visualized by the deconvolution of the curves (See Figures S9–S12, supplementary materials). Zinc(II) and cadmium(II) cations (as well as the other metal cations with complete electron shell configuration) are known not to interfere with the ligand-centered luminescence [48], therefore, these two components could be assigned to the terephthalate anion and the imidazolyl moiety, respectively [49,50]. The position of the luminescence emission spectra peak for

terephthalate anion is consistent among all four compounds (423–430 nm). The position of the peak of the emission spectra for imidazolyl group depends on the alkyl chain length. For compounds **1** and **2** with shorter C5 ligand it centers near 543–546 nm. For compounds **3** and **4** with longer C6 ligand the luminescence maximum is located at 484–488 nm. Such difference should be attributed to a change of the HOMO–LUMO energy levels of the imidazolyl moieties, separated by a different number of the methylene groups in the alkyl chain. It should be noted, that according to literature data, free imidazolyl ligands demonstrate emission maxima around 495 nm [24].

The comparison of the luminescence spectra prompts a number of interesting observations and conclusions. First of all, metal cation does not seem to have an effect on the shape of both excitation and emission spectra. However, a twice greater luminescence intensity for zinc-containing compounds (**1** and **3**), compared to the corresponding cadmium compounds (**2** and **4**), implies that the Zn^{2+} increases the probability of the electron transitions between ligand molecular orbitals, compared to Cd^{2+}. Very interestingly, the length of the alkyl chain greatly affects the relative intensity of the luminescence as well as the ratio between the terephthalate and the imidazolyl components of the spectra. The coordination structures **1** and **2** with pentamethylene chains feature significantly higher intensity of the emission of the imidazolyl component, compared to that of terephthalate. On the contrary, the relative luminescence intensities of both the terephthalate and imidazolyl moieties in **3** and **4**, containing hexamethylene chain, are comparable. At this point, it is hard to explain how one methylene group affects the luminescence properties so much. Clearly, detailed spectroscopic studies of the quantum yields and luminescence lifetimes as well as quantum chemical calculations should provide the missing insights on the luminescence properties of the title compounds. Lastly, the crystal structure of the building unit as well as the network topology in **4** does have little effect (if at all) on its luminescence. As it was mentioned above, the differences should be attributed to the chemical composition of the compounds, rather than to the topology of the coordination networks.

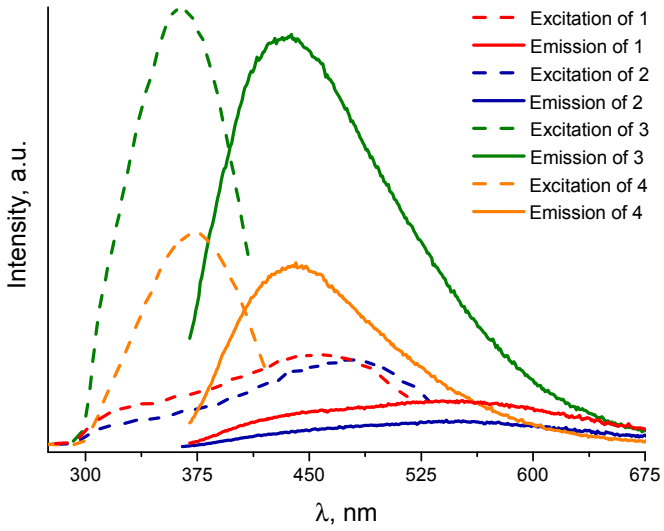

Figure 10. Excitation and emission luminescence spectra of the compounds **1**–**4**.

3. Materials and Methods

All reagents and solvents were commercially available and used as supplied without further purification.

The FTIR spectra were recorded from KBr pellets in the range 4000–400 cm^{-1} on Scimitar FTS 2000 Fourier-transform infrared spectrometer. Thermogravimetric analysis (TGA) were performed using TG 209 F1 Iris Thermo Microbalance (NETZSCH) instrument at temperatures between 25 and 600 °C in He atmosphere and heating rate 10 °C/min. Powder X-ray diffraction (PXRD) patterns were measured with Cu-K_α radiation on a Phillips PW 1830 instrument equipped with a vertical

Bragg-Bretano powder goniometer and a PW 1710 control unit. Elemental analyses (C, H, N) were performed on the Euro EA CHN Elemental Analyzer. NMR spectra were recorded on Bruker AV300 instrument operating at 300 MHz for ^{1}H and 75 MHz for ^{13}C. The luminescence spectra were recorded on Horiba Jobin Yvon Fluorolog 3 Photoluminescence Spectrometer, equipped by 450 W xenon lamp, excitation/emission monochromator, and FL-1073 PMT detector.

Diffraction data for single crystals of compound **1** and **2** were obtained at 130 K on an automated Agilent Xcalibur diffractometer equipped with a CCD AtlasS2 detector (MoKα, graphite monochromator, ω-scans). Diffraction data for a single crystal of compound **3** and **4** were obtained at 120 K on an automated Agilent GV1000 diffractometer equipped with a CCD AtlasS2 detector (CuKα, rotating anode, ω-scans). Integration, absorption correction, and determination of unit cell parameters were performed using the CrysAlisPro program package [51]. The structures were solved by a direct method and refined by the full-matrix least squares technique in the anisotropic approximation (except hydrogen atoms) using the SHELX-2014 software package [52]. Positions of hydrogen atoms of organic spices were calculated geometrically and refined in the riding model. The data given for **3** are the best we could achieve. Despite our hardest efforts, we were able to isolate only small crystals of the compound which gave modest diffraction. The values of the ratio $I/\sigma(I)$ at a resolution higher than 1.0 does not exceed 4 ($R_{int} > 0.40$). Thus, we were not able to establish a complete crystal structure of a compound **3** that would meet all quality criteria. However, the structure of the metal-organic framework including the local coordination geometry of Zn(II) cations, the conformation of the organic ligand, as well as the connectivity and topology of the coordination network are reliably determined. The crystallographic data and details of the structure refinements are summarized in Table 1. Selected geometric parameters of molecular structures **1**–**4** are listed in Table 2.

Table 1. Crystal data and structure refinement for **1**–**4**.

Compound	1	2	3	4
Empirical formula	$C_{22}H_{27}N_5O_5Zn$	$C_{22}H_{27}CdN_5O_5$	$C_{20}H_{22}N_4O_4Zn$	$C_{21}H_{26}CdN_4O_5$
M, g/mol	506.85	553.88	447.78	526.86
T, K	130(2)	130(2)	120(2)	120(2)
λ, Å	0.71073 (MoKα)	0.71073 (MoKα)	1.54184 (CuKα)	1.54184 (CuKα)
Crystal system	Monoclinic	Monoclinic	Orthorhombic	Triclinic
Space group	$P2_1/c$	$P2_1/c$	$P2_12_12_1$	$P-1$
a, Å	10.73257(16)	10.8546(3)	15.123(5)	9.2444(10)
b, Å	23.2562(3)	23.6261(7)	18.806(5)	10.0116(8)
c, Å	9.76351(17)	9.6799(3)	20.722(4)	14.4659(13)
α, deg.	90	90	90	107.371(8)
β, deg.	105.3925(17)	104.140(3)	90	91.269(8)
γ, deg.	90	90	90	116.622(10)
V, Å^3	2349.55(6)	2407.21(13)	5893(3)	1123.1(2)
Z	4	4	12	2
D(calcd.), g/cm^3	1.433	1.528	1.514	1.558
μ, mm^{-1}	1.088	0.949	2.038	8.124
F(000)	1056	1128	2784	536
Crystal size, mm	0.34 × 0.31 × 0.21	0.88 × 0.15 × 0.13	0.10 × 0.04 × 0.04	0.42 × 0.23 × 0.06
θ range for data collection, deg.	3.40–30.99	3.36–31.14	3.62–70.07	5.15–74.36
Index ranges	$-15 \le h \le 14$, $-32 \le k \le 32$, $-14 \le l \le 9$	$-15 \le h \le 15$, $-32 \le k \le 31$, $-13 \le l \le 11$	$-17 \le h \le 18$, $-22 \le k \le 22$, $-25 \le l \le 15$	$-11 \le h \le 11$, $-10 \le k \le 12$, $-17 \le l \le 15$
Reflections collected/independent	24131/6791	24703/6948	15255/9867	8600/4465
R_{int}	0.0160	0.0184	0.1258	0.0568
Reflections with $I > 2\sigma(I)$	6249	6270	5058	4272
Goodness-of-fit on F^2	1.075	1.090	1.760	1.055
Final *R* indices [$I > 2\sigma(I)$]	$R_1 = 0.0374$, $wR_2 = 0.1059$	$R_1 = 0.0268$, $wR_2 = 0.0607$	$R_1 = 0.1719$, $wR_2 = 0.4597$	$R_1 = 0.0487$, $wR_2 = 0.1236$
R indices (all data)	$R_1 = 0.0409$, $wR_2 = 0.1082$	$R_1 = 0.0317$, $wR_2 = 0.0628$	$R_1 = 0.2661$, $wR_2 = 0.5394$	$R_1 = 0.0503$, $wR_2 = 0.1292$
Largest diff. peak/hole, e/Å^3	1.227/−0.532	1.584/−0.379	3.392/−3.531	1.790/−1.490

Table 2. Selected bond lengths and angles for **1**–**4**.

Compound 1			
Bond	***d*, Å**	**Bond**	***d*, Å**
Zn(1)–O(11)	1.9581(14)	Zn(1)–N(11)	2.0273(16)
Zn(1)–O(21)	1.9714(12)	Zn(1)–N(14) [i]	1.9987(15)
Angle	**ω, deg.**	**Angle**	**ω, deg.**
O(11)–Zn(1)–O(21)	102.79(7)	O(21)–Zn(1)–N(11)	117.80(6)
O(11)–Zn(1)–N(11)	93.57(7)	O(21)–Zn(1)–N(14) [i]	112.02(6)
O(11)–Zn(1)–N(14) [i]	125.78(6)	N(14) [i]–Zn(1)–N(11)	104.57(6)
Symmetry transformations used to generate equivalent atoms: (i) $x-1, -y+\frac{1}{2}, z-\frac{1}{2}$.			
Compound 2			
Bond	***d*, Å**	**Bond**	***d*, Å**
Cd(1)–O(11)	2.2782(12)	Cd(1)–O(22)	2.4000(13)
Cd(1)–O(12)	2.4848(13)	Cd(1)–N(11)	2.2561(15)
Cd(1)–O(21)	2.3262(12)	Cd(1)–N(14) [i]	2.2355(14)
Angle	**ω, deg.**	**Angle**	**ω, deg.**
O(11)–Cd(1)–O(12)	55.05(4)	N(11)–Cd(1)–O(21)	84.42(5)
O(11)–Cd(1)–O(21)	91.19(5)	N(11)–Cd(1)–O(22)	111.99(5)
O(11)–Cd(1)–O(22)	106.26(5)	N(14) [i]–Cd(1)–O(11)	112.06(5)
O(21)–Cd(1)–O(12)	126.27(4)	N(14) [i]–Cd(1)–O(12)	89.67(5)
O(21)–Cd(1)–O(22)	55.49(4)	N(14) [i]–Cd(1)–O(21)	144.03(5)
O(22)–Cd(1)–O(12)	159.54(5)	N(14) [i]–Cd(1)–O(22)	90.73(5)
N(11)–Cd(1)–O(11)	129.33(5)	N(14) [i]–Cd(1)–N(11)	99.61(5)
N(11)–Cd(1)–O(12)	88.08(5)		
Symmetry transformations used to generate equivalent atoms: (i) $x-1, -y+\frac{1}{2}, z-\frac{1}{2}$.			
Compound 3			
Bond	***d*, Å**	**Bond**	***d*, Å**
Zn(1)–O(11)	2.03(3)	Zn(2)–O(23) [ii]	1.95(2)
Zn(1)–N(11)	2.05(2)	Zn(2)–N(24) [iii]	1.99(3)
Zn(1)–O(22)	2.12(3)	Zn(3)–N(14)	2.05(3)
Zn(1)–N(34) [i]	1.98(2)	Zn(3)–O(31)	1.98(2)
Zn(2)–O(13)	1.94(3)	Zn(3)–N(31)	1.99(2)
Zn(2)–N(21)	2.01(3)	Zn(3)–O(34) [iv]	1.99(3)
Angle	**ω, deg.**	**Angle**	**ω, deg.**
O(11)–Zn(1)–N(11)	105.1(14)	O(23) [ii]–Zn(2)–N(21)	108.3(14)
O(11)–Zn(1)–O(22)	120.9(11)	O(23) [ii]–Zn(2)–N(24) [iii]	109.7(14)
N(11)–Zn(1)–O(22)	97.4(14)	N(24) [iii]–Zn(2)–N(21)	112.5(10)
N(34) [i]–Zn(1)–O(11)	111.6(15)	O(31)–Zn(3)–N(14)	110.4(11)
N(34) [i]–Zn(1)–N(11)	112.1(9)	O(31)–Zn(3)–N(31)	114.5(11)
N(34) [i]–Zn(1)–O(22)	108.8(15)	O(31)–Zn(3)–O(34) [iv]	115.6(9)
O(13)–Zn(2)–N(21)	114.4(13)	N(31)–Zn(3)–N(14)	111.8(9)
O(13)–Zn(2)–N(24) [iii]	98.5(14)	N(31)–Zn(3)–O(34) [iv]	109.7(11)
O(13)–Zn(2)–O(23) [ii]	113.3(10)	O(34) [iv]–Zn(3)–N(14)	92.8(12)
Symmetry transformations used to generate equivalent atoms: (i) $x+1, y, z$; (ii) $x, y+1, z$; (iii) $x+1/2, -y+3/2, -z$; (iv) $-x+1, y+\frac{1}{2}, -z+5/2$.			
Compound 4			
Bond	***d*, Å**	**Bond**	***d*, Å**
Cd(1)–O(11)	2.399(3)	Cd(1)–O(22) [i]	2.216(3)
Cd(1)–O(12)	2.446(3)	Cd(1)–N(11)	2.324(4)
Cd(1)–O(21)	2.287(3)	Cd(1)–N(21)	2.259(3)
Angle	**ω, deg.**	**Angle**	**ω, deg.**
O(11)–Cd(1)–O(12)	54.22(9)	O(22) [i]–Cd(1)–N(21)	108.86(11)
O(21)–Cd(1)–O(11)	90.18(10)	N(11)–Cd(1)–O(11)	83.89(11)
O(21)–Cd(1)–O(12)	86.53(10)	N(11)–Cd(1)–O(12)	91.99(12)
O(21)–Cd(1)–N(11)	173.57(11)	N(21)–Cd(1)–O(11)	110.33(11)
O(22) [i]–Cd(1)–O(11)	139.13(10)	N(21)–Cd(1)–O(12)	164.17(12)
O(22) [i]–Cd(1)–O(12)	86.97(10)	N(21)–Cd(1)–O(21)	90.41(11)
O(22) [i]–Cd(1)–O(21)	100.73(10)	N(21)–Cd(1)–N(11)	89.32(13)
O(22) [i]–Cd(1)–N(11)	85.42(12)		
Symmetry transformations used to generate equivalent atoms: (i) $-x+2, -y+1, -z$.			

1,5-Bis(imidazol-1-yl)pentane (**C5**). A suspension of 1.36 g (20 mmol) of imidazole, 1.68 g (30 mmol) of powdered KOH in 5 mL of DMSO was vigorously stirred at 80 °C during 30 min. The reaction flask was then immersed in a cold water bath and, after cooling to room temperature, 2.30 g (10 mmol) of 1,5-dibromopentane in 5 mL of DMSO was added dropwise during 30 min. After the addition was completed, the reaction mixture was stirred and refluxed overnight, then it was quenched with 200 mL of water and evaporated in vacuum on a rotary evaporator. The resulting viscous residue was treated by ethyl acetate to extract the product. Removal on ethyl acetate gave the product as light-yellow oil. Yield 88%. IR bands (cm^{-1}): 1578, 1466, 1433, 1430 (Im). NMR ^1H ($CDCI_3$), δ, ppm: 1.05 (q, 2H, $ImCH_2CH_2\underline{CH_2}$, J 7.5 Hz), 1.56 (q, 4H, $ImCH_2\underline{CH_2}CH_2$, J 7.5 Hz), 3.67 (t, 4H, $Im\underline{CH_2}CH_2CH_2$, J 7.5 Hz), 6.66 (2H, H^4-Im), 6.78 (2H, H^5-Im), 7.20 (2H, H^2-Im). NMR ^{13}C ($CDCI_3$), δ, ppm: 22.9 ($ImCH_2CH_2\underline{CH_2}$), 29.8 ($ImCH_2\underline{CH_2}CH_2$), 46.0 ($Im\underline{CH_2}CH_2CH_2$), 118.2 (Im-$C^5$), 128.5 (Im-$C^4$), 136.4 (Im-$C^2$).

1,6-Bis(imidazol-1-yl)hexane (**C6**) was prepared similarly to compound C5 using 1,6-dibromohexane as alkylating agent. Yield 86%. IR bands (cm^{-1}): 1562, 1507, 1462, 1349 (Im). NMR ^1H ($CDCI_3$), δ, ppm: 0.97 (q, 4H, $ImCH_2CH_2\underline{CH_2}$, J 6.5 Hz), 1.43 (q, 4H, $ImCH_2\underline{CH_2}CH_2$, J 6.5 Hz), 3.59 (t, 4H, $Im\underline{CH_2}CH_2CH_2$, J 6.5 Hz), 6.60 (2H, H^4-Im), 6.71 (2H, H^5-Im), 7.14 (2H, H^2-Im). NMR ^{13}C ($CDCI_3$), δ, ppm: 25.0 ($ImCH_2CH_2\underline{CH_2}$), 30.2 ($ImCH_2\underline{CH_2}CH_2$), 46.1 ($Im\underline{CH_2}CH_2CH_2$), 118.0 (Im-$C^5$), 128.5 (Im-$C^4$), 136.5 (Im-$C^2$).

Synthesis of [Zn(bdc)(C5)]·$DMF_{0,6}$·$H_2O_{0,4}$ (**1**): A mixture of $Zn(NO_3)_2·6H_2O$ (30 mg, 0.1 mmol), terephthalic acid (17 mg, 0.1 mmol), C5 (18.5 μL, 0.11 mmol) and DMF (4 mL) was mixed and heated at 100 °C for 24 h in a screwed-cap glass vial. The obtained brownish crystals were filtered, washed with DMF (1 mL, three times) and dried in air flow for 10 min. Yield: 43 mg (89% based on Zn). Elemental analyses. Calculated for $C_{20,8}H_{25,2}N_{4,6}O_{5,1}Zn$ (%): C 51.5; H 5.2; N 13.3. Found (%): C 51.2; H 5.3; N 13.3. TG analysis. Found: 10% solvent weight loss. Calculated for 0.6(DMF) + 0.4(H_2O): 10%. IR bands (cm^{-1}): 3450 (w), 3125 (m), 3055 (w), 2942 (m), 2864 (w), 1956 (w), 1605 (s), 1532 (m), 1500 (m), 1455 (m), 1348 (s), 1236 (s), 1095 (s), 1015 (m), 955 (s), 826 (s), 749 (s), 656 (s), 629 (m), 570 (m), 514 (m).

Synthesis of [Cd(bdc)(C5)]·DMF (**2**): $Cd(NO_3)_2·4H_2O$ (31 mg, 0.1 mmol), terephthalic acid (17 mg, 0.1 mmol), and C5 (18.5 μL, 0.11 mmol) were mixed in methanol (2 mL) and DMF (2 mL) and heated at 100 °C for 24 h in a screwed-cap glass vial. The obtained colorless crystals were filtered, washed with DMF (1 mL, three times) and dried in air flow for 10 min. Yield: 46 mg (83% based on Cd). Elemental analysis. Calculated for $C_{22}H_{27}CdN_5O_5$ (%): C 47.7; H 4.9; N 12.6. Found (%): C 47.7; H 5.2; N 12.7. TG analysis. Found: 13% solvent weight loss. Calculated for 1(DMF): 13%. IR bands (cm^{-1}): 3422 (w), 3110 (m), 2939 (m), 2864 (w), 1670 (s), 1560 (s), 1527 (m), 1444 (m), 1388 (s), 1296 (m), 1236 (m), 1098 (s), 1014 (w), 943 (m), 890 (w), 837 (s), 753 (s), 657 (s), 526 (s).

Synthesis of [Zn(bdc)(C6)] (**3**): A mixture of $Zn(NO_3)_2·6H_2O$ (30 mg, 0.1 mmol), terephthalic acid (17 mg, 0.1 mmol), and C6 (20 μL, 0.11 mmol) were mixed in methanol (2 mL) and DMF (2 mL) and heated at 100 °C for 24 h in a screwed-cap glass vial. The obtained colorless crystals were filtered, washed with DMF (1 mL, three times) and dried in air flow for 10 min. Yield: 32 mg (71% based on Zn). Elemental analysis. Calculated for $C_{20}H_{22}N_4O_4Zn$ (%): C 53.6; H 5.0; N 12.5. Found (%): C 53.0; H 5.0; N 12.5. IR bands (cm^{-1}): ν = 3446 (w), 3122 (m), 3050 (w), 2948 (m), 2868 (w), 1952 (w), 1604 (s), 1528 (m), 1498 (m), 1454 (w), 1353 (s), 1243 (m), 1110 (s), 952 (m), 886 (w), 826 (s), 757 (s), 656 (s), 622 (w), 583 (w), 517 (w).

Synthesis of [Cd(bdc)(C6)]·MeOH (**4**): The compound was prepared similarly to **2**, using C6 ligand (20 μL, 0.11 mmol) instead of C5. Yield: 41 mg (78% based on Cd). Elemental analysis. Calculated for $C_{21}H_{26}CdN_4O_5$ (%): C 47.9; H 5.0; N 10.6. Found (%): C 48.2; H 4.7; N 11.0. TG analysis: Found: 6% solvent weight loss. Calculated for 1(MeOH): 6%. IR bands (cm^{-1}): 3411 (m), 3129 (m), 3046 (w), 2936 (m), 2861 (w), 2817 (w), 1855 (w), 1562 (s), 1522 (m), 1446 (m), 1379 (s), 1293 (m),1237 (m), 1090 (s), 1035 (m), 939 (m), 888 (w), 835 (s), 751 (s), 657 (s), 557 (w), 517 (m).

4. Conclusions

In summary, we reported the new convenient multi-gram scale synthesis of two bisimidazolyl molecules with flexible nature and four coordination polymers based on these molecules, Zn(II)/Cd(II) cations as well as terephthalate ligands. Three compounds feature very common four-connected diamond-like topology (**dia**), which could be anticipated, contrary to the other compound with a very rare **ilc** topology based on eight-connected nodes. All compounds feature ligand-based luminescence properties in the solid state with two independent emission sources. The detailed analysis of the luminescence spectra reveals the major influence of the chemical composition on the optical properties of the materials. Strikingly, the experimental data indicate that varying of the length of the alkyl chain of bis(imidazole) ligand by just one methylene unit greatly affects the relative luminescence intensity of the terephthalate anion compared to that of imidazolyl moiety.

Supplementary Materials: The following are available online at http://www.mdpi.com/2073-4352/6/10/132/s1, Figure S1: Experimental and calculated XDR pattern for compound **1**, Figure S2: Experimental and calculated XDR pattern for compound **2**, Figure S3: Experimental and calculated XDR pattern for compound **3**, Figure S4: Experimental and calculated XDR pattern for compound **4**, Figure S5: Thermogravimetric curve for compound **1**, Figure S6: Thermogravimetric curve for compound **2**, Figure S7: Thermogravimetric curve for compound **3**, Figure S8: Thermogravimetric curve for compound **4**, Figure S9: The experimental emission spectra of compound **1** and its deconvolution onto two components, Figure S10: The experimental emission spectra of compound **2** and its deconvolution onto two components, Figure S11: The experimental emission spectra of compound **3** and its deconvolution onto two components, Figure S12: The experimental emission spectra of compound **4** and its deconvolution onto two components, Figure S13: The emission luminescence spectra of the coordination polymers **1**–**4** with normalized intensities. Crystallographic data for the structural analysis have been deposited with the Cambridge Crystallographic Data Centre, CCDC Nos. 1436875-1436878 for **1**, **2**, **3,** and **4**. Copies of the data can be obtained free of charge from the Cambridge Crystallographic Data Centre, 12 Union Road, Cambridge CB2 1EZ, UK (fax: +44-1223-336-033; e-mail:deposit@ccdc.cam.ac.uk).

Acknowledgments: The reported study was supported by the Russian Science Foundation, Grant No. 15-13-10023. The authors are grateful to M.I. Rakhmanova for luminescence measurements and V.D. Orogodnikov for recording NMR spectra.

Author Contributions: Danil Dybtsev and Andrei Potapov conceived and designed the experiments, Marina Barsukova and Tatiana Goncharova carried out the synthesis, Denis Samsonenko performed X-ray structure determination and analyzed the results.

Conflicts of Interest: The authors declare no conflict of interest. The founding sponsors had no role in the design of the study; in the collection, analyses, or interpretation of data; in the writing of the manuscript, and in the decision to publish the results.

References

1. Eddaoudi, M.; Kim, J.; Rosi, N.; Vodak, D.; Wachter, J.; O'Keeffe, M.; Yaghi, O.M. Systematic design of pore size and functionality in isoreticular MOFs and their application in methane storage. *Science* **2002**, *295*, 469–472. [CrossRef] [PubMed]
2. Li, J.-R.; Kuppler, R.J.; Zhou, H.-C. Selective gas adsorption and separation in metal-organic frameworks. *Chem. Soc. Rev.* **2009**, *38*, 1477–1504. [CrossRef] [PubMed]
3. Sumida, K.; Rogow, D.L.; Mason, J.A.; McDonald, T.M.; Bloch, E.D.; Herm, Z.R.; Bae, T.-H.; Long, J.R. Carbon dioxide capture in metal-organic frameworks. *Chem. Rev.* **2012**, *112*, 724–781. [CrossRef] [PubMed]
4. Adatoz, E.; Avci, A.K.; Keskin, S. Opportunities and challenges of MOF-based membranes in gas separations. *Sep. Purif. Technol.* **2015**, *152*, 207–237. [CrossRef]
5. Lai, Q.; Paskevicius, M.; Sheppard, D.A.; Buckley, C.E.; Thornton, A.W.; Hill, M.R.; Gu, Q.; Mao, J.; Huang, Z.; Liu, H.K.; et al. Hydrogen Storage Materials for Mobile and Stationary Applications: Current State of the Art. *ChemSusChem* **2015**, *8*, 2789–2825. [CrossRef] [PubMed]
6. Butova, V.V.; Soldatov, M.A.; Guda, A.A.; Lomachenko, K.A.; Lamberti, C. Metal-organic frameworks: Structure, properties, synthesis and characterization. *Russ. Chem. Rev.* **2016**, *85*, 280–307. [CrossRef]
7. Cui, Y.; Yue, Y.; Qian, G.; Chen, B. Luminescent functional metal-organic frameworks. *Chem. Rev.* **2012**, *112*, 1126–1162. [CrossRef] [PubMed]
8. Feng, C.; Ma, Y.-H.; Zhang, D.; Li, X.-J.; Zhao, H. Highly efficient electrochemiluminescence based on pyrazolecarboxylic metal organic framework. *Dalton Trans.* **2016**, *45*, 5081–5091. [CrossRef] [PubMed]

9. Mendiratta, S.; Lee, C.-H.; Usman, M.; Lu, K.-L. Metal-organic frameworks for electronics: Emerging second order nonlinear optical and dielectric materials. *Sci. Technol. Adv. Mater.* **2016**, *16*, 54204. [CrossRef]
10. Tai, X.-S.; You, H.-Y. A New 1D Chained Coordination Polymer: Synthesis, Crystal Structure, Antitumor Activity and Luminescent Property. *Crystals* **2015**, *5*, 608–616. [CrossRef]
11. Kreno, L.E.; Leong, K.; Farha, O.K.; Allendorf, M.; Van Duyne, R.P.; Hupp, J.T. Metal-organic framework materials as chemical sensors. *Chem. Rev.* **2012**, *112*, 1105–1125. [CrossRef] [PubMed]
12. Chughtai, A.H.; Ahmad, N.; Younus, H.A.; Laypkov, A.; Verpoort, F. Metal-organic frameworks: Versatile heterogeneous catalysts for efficient catalytic organic transformations. *Chem. Soc. Rev.* **2015**, *44*, 6804–6849. [CrossRef] [PubMed]
13. Alegre-Requena, J.V.; Marques-Lopez, E.; Herrera, R.P.; Diaz, D.D. Metal-organic frameworks (MOFs) bring new life to hydrogen-bonding organocatalysts in confined spaces. *CrystEngComm* **2016**, *18*, 3985–3995. [CrossRef]
14. Cai, W.; Chu, C.-C.; Liu, G.; Wáng, Y.-X.J. Metal-Organic Framework-Based Nanomedicine Platforms for Drug Delivery and Molecular Imaging. *Small* **2015**, *11*, 4806–4822. [CrossRef] [PubMed]
15. Mehta, J.; Bhardwaj, N.; Bhardwaj, S.K.; Kim, K.-H.; Deep, A. Recent advances in enzyme immobilization techniques: Metal-organic frameworks as novel substrates. *Coord. Chem. Rev.* **2016**, *322*, 30–40. [CrossRef]
16. Lu, W.; Wei, Z.; Gu, Z.Y.; Liu, T.F.; Park, J.; Park, J.; Tian, J.; Zhang, M.; Zhang, Q.; Gentle Iii, T.; et al. Tuning the structure and function of metal-organic frameworks via linker design. *Chem. Soc. Rev.* **2014**, *43*, 5561–5593. [CrossRef] [PubMed]
17. Lin, Z.-J.; Lü, J.; Hong, M.; Cao, R. Metal-organic frameworks based on flexible ligands (FL-MOFs): Structures and applications. *Chem. Soc. Rev.* **2014**, *43*, 5867–5895. [CrossRef] [PubMed]
18. Pettinari, C.; Tăbăcaru, A.; Galli, S. Coordination Polymers and Metal-Organic Frameworks Based on Poly(pyrazole)-containing Ligands. *Coord. Chem. Rev.* **2016**, *307*, 1–31. [CrossRef]
19. Pettinari, C.; Pettinari, R. Metal derivatives of poly(pyrazolyl)alkanes: II. Bis(pyrazolyl)alkanes and related systems. *Coord. Chem. Rev.* **2005**, *249*, 663–691. [CrossRef]
20. Tahli, A.; Köc, Ü.; Elshaarawy, R.; Kautz, A.; Janiak, C. A Cadmium Anionic 1-D Coordination Polymer $\{[Cd(H_2O)_6][Cd_2(atr)_2(\mu^2\text{-btc})_2(H_2O)_4]\ 2H_2O\}_n$ within a 3-D Supramolecular Charge-Assisted Hydrogen-Bonded and π-Stacking Network. *Crystals* **2016**, *6*, 23. [CrossRef]
21. Zhang, L.-P.; Wen, S.-T.; Fu, X.-N. *catena*-Poly[[[diaqua-copper(II)]-bis-[μ-1,5-bis-(1H-imidazol-1-yl)pentane-κ(2) N (3):N (3′)]] naphthalene-1,5-disulfonate]. *Acta Crystallogr. Sect. E. Struct. Rep. Online* **2012**, *68*, m1505. [CrossRef] [PubMed]
22. Zhang, W.-L.; Liu, Y.-Y.; Ma, J.-F.; Jiang, H.; Yang, J. Syntheses and characterizations of nine coordination polymers of transition metals with carboxylate anions and bis(imidazole) ligands. *Polyhedron* **2008**, *27*, 3351–3358. [CrossRef]
23. Li, X.-Y.; Liu, M.; Yue, K.-F.; Wu, Y.-P.; He, T.; Yan, N.; Wang, Y.-Y. A series of reaction-controlled coordination polymers constructed from bis(imidazole) and tetrafluoroterephthalic acid ligands: Syntheses, structural diversities, properties. *CrystEngComm* **2015**, *17*, 8273–8281. [CrossRef]
24. Zheng, L.-Y.; Zhao, S.; Liu, L.; Li, K.; Li, B.-L.; Wu, B. Syntheses, structures and luminescence of two cadmium entangled coordination polymers based on bis(imidazole) and biscarboxylate ligands. *Inorg. Chem. Commun.* **2015**, *57*, 84–88. [CrossRef]
25. Zhang, J.; Yang, J.; Wang, X.; Zhang, H.; Chi, X.; Yang, Q.; Chen, Y.; Xiao, D. A series of polythreaded architectures based on a long flexible tetracarboxylate ligand and different N-donor ligands. *Inorg. Chim. Acta* **2016**, *447*, 66–76. [CrossRef]
26. Zhang, F.-L.; Tian, L.; Qin, L.-F.; Chen, J.-Q.; Li, Z.; Ren, X.; Gu, Z.-G. Chiral double helical silver complexes: Subcomponent self-assembly and self-sorting. *Polyhedron* **2016**, *104*, 9–16. [CrossRef]
27. Wu, W.P.; Wang, J.; Lu, L.; Wu, Y. Syntheses and luminescence of four supramolecular coordination complexes with flexible ligand. *Russ. J. Coord. Chem.* **2016**, *42*, 217–224. [CrossRef]
28. Cheng, H.-J.; Tang, X.-Y.; Yuan, R.-X.; Lang, J.-P. Structural diversity of Zn(II) coordination polymers based on bis-imidazolyl ligands and 5-R-1,3-benzenedicarboxylate and their photocatalytic properties. *CrystEngComm* **2016**, *18*, 4851–4862. [CrossRef]
29. Lu, J.-F.; Liu, Z.-H. Three metal induced 3D coordination polymers based on H3BTC and 1,3-BIP as co-ligands: Synthesis, structures and fluorescent properties. *Polyhedron* **2016**, *107*, 19–26. [CrossRef]

30. Zheng, L.-Y.; Li, K.; Zhao, S.; Liu, L.; Li, B.-L.; Wu, B. Syntheses, structures and properties of eight coordination polymers based on bis(imidazole) and biscarboxylate ligands. *Polyhedron* **2016**, *104*, 1–8. [CrossRef]
31. Yang, Z.; Han, S.-S.; Zheng, L.-Y.; Peng, Y.-F.; Li, B.-L.; Li, H.-Y. Syntheses, structures, and properties of two- and three-dimensional coordination polymers based on bis(imidazole) and glutarate ligands. *J. Coord. Chem.* **2015**, *68*, 1213–1223. [CrossRef]
32. Chen, S.-S. The roles of imidazole ligands in coordination supramolecular systems. *CrystEngComm* **2016**, *18*, 6543–6565. [CrossRef]
33. Sharma, S.K.; Tandon, M.; Lown, J.W. Design and Synthesis of Novel Thiazole-Containing Cross-Linked Polyamides Related to the Antiviral Antibiotic Distamycin. *J. Org. Chem.* **2000**, *65*, 1102–1107. [CrossRef] [PubMed]
34. Shoji, O.; Okada, S.; Satake, A.; Kobuke, Y. Coordination assembled rings of ferrocene-bridged trisporphyrin with flexible hinge-like motion: Selective dimer ring formation, its transformation to larger rings, and vice versa. *J. Am. Chem. Soc.* **2005**, *127*, 2201–2210. [CrossRef] [PubMed]
35. Pandey, J.; Tiwari, V.K.; Verma, S.S.; Chaturvedi, V.; Bhatnagar, S.; Sinha, S.; Gaikwad, A.N.; Tripathi, R.P. Synthesis and antitubercular screening of imidazole derivatives. *Eur. J. Med. Chem.* **2009**, *44*, 3350–3355. [CrossRef] [PubMed]
36. Kumar, S.; Gupta, S.K. The first examples of discotic liquid crystalline gemini surfactants. *Tetrahedron Lett.* **2010**, *51*, 5459–5462. [CrossRef]
37. Yang, M.; Stappert, K.; Mudring, A.-V. Bis-cationic ionic liquid crystals. *J. Mater. Chem. C* **2014**, *2*, 458–473. [CrossRef]
38. Gao, Y.; Slattery, J.M.; Bruce, D.W. Columnar thermotropic mesophases formed by dimeric liquid-crystalline ionic liquids exhibiting large mesophase ranges. *New J. Chem.* **2011**, *35*, 2910–2918. [CrossRef]
39. Potapov, A.S.; Nudnova, E.A.; Khlebnikov, A.I.; Ogorodnikov, V.D.; Petrenko, T.V. Synthesis of new polydentate pyrazolyl-ethene ligands by interaction of 1H-pyrazole and 1,1,2,2-tetrabromoethane in a superbasic medium. *J. Heterocycl. Chem.* **2011**, *48*, 645–651. [CrossRef]
40. Domina, G.A.; Potapov, A.S.; Khlebnikov, A.I.; Ogorodnikov, V.D. Synthesis of 1,8-di(pyrazol-1-yl)-3,6-dioxaoctane and its derivatives. *Russ. J. Org. Chem.* **2009**, *45*, 1224–1228. [CrossRef]
41. Spek, A.L. Structure validation in chemical crystallography. *Acta Crystallogr. D Biol. Crystallogr.* **2009**, *65*, 148–155. [CrossRef] [PubMed]
42. Wang, X.-L.; Qin, C.; Wang, E.-B.; Su, Z.-M.; Xu, L.; Batten, S.R. An unprecedented eight-connected self-penetrating network based on pentanuclear zinc cluster building blocks. *Chem. Commun.* **2005**, *38*, 4789–4791. [CrossRef] [PubMed]
43. Qiblawi, S.H.; Sposato, L.K.; LaDuca, R.L. Chain, layer, and self-penetrated copper dipyridylamine coordination polymers with conformationally flexible ring-based dicarboxylate ligands. *Inorg. Chim. Acta* **2013**, *407*, 297–305. [CrossRef]
44. Wang, D.; Zhang, L.; Li, G.; Huo, Q.; Liu, Y. Luminescent MOF material based on cadmium(II) and mixed ligands: Application for sensing volatile organic solvent molecules. *RSC Adv.* **2015**, *5*, 18087–18091. [CrossRef]
45. Farnum, G.A.; Lucas, J.S.; Wang, C.Y.; LaDuca, R.L. Luminescent cadmium and zinc diphenate coordination polymers containing pyridyl-piperazine type ligands: Grids, diamondoid lattices, and a rare 4-connected net. *Inorg. Chim. Acta* **2011**, *368*, 84–95. [CrossRef]
46. Yang, P.-P.; Li, B.; Wang, Y.-H.; Gu, W.; Liu, X. Synthesis, Structure, and Luminescence Properties of Zinc(II) and Cadmium(II) Complexes containing the Flexible Ligand of 3,3′-Thiodipropionic Acid. *Z. Anorg. Allg. Chem.* **2008**, *634*, 1221–1224. [CrossRef]
47. Bushuev, M.B.; Selivanov, B.A.; Pervukhina, N.V.; Naumov, D.Y.; Rakhmanova, M.I.; Sheludyakova, L.A.; Tikhonov, A.Y.; Larionov, S.V. Luminescent zinc(II) and cadmium(II) complexes based on 2-(4,5-dimethyl-1H-imidazol-2-yl)pyridine and 2-(1-hydroxy-4,5-dimethyl-1H-imidazol-2-yl)pyridine. *Russ. J. Gen. Chem.* **2012**, *82*, 1859–1868. [CrossRef]
48. Heine, J.; Müller-Buschbaum, K. Engineering metal-based luminescence in coordination polymers and metal–organic frameworks. *Chem. Soc. Rev.* **2013**, *42*, 9232–9242. [CrossRef] [PubMed]

49. Sapchenko, S.A.; Dybtsev, D.N.; Samsonenko, D.G.; Fedin, V.P. Synthesis, crystal structures, luminescent and thermal properties of two new metal–organic coordination polymers based on zinc(II) carboxylates. *New J. Chem.* **2010**, *34*, 2445–2450. [CrossRef]
50. Wei, G.-H.; Yang, J.; Ma, J.-F.; Liu, Y.-Y.; Li, S.-L.; Zhang, L.-P. Syntheses, structures and luminescent properties of zinc(II) and cadmium(II) coordination complexes based on new bis(imidazolyl)ether and different carboxylate ligands. *Dalt. Trans.* **2008**, *127*, 3080–3092. [CrossRef] [PubMed]
51. CrysAlisPro, Version 1.171.34.49 (release 20-01-2011 CrysAlis171 .NET). Agilent Technologies: Santa Clara, CA, USA.
52. Sheldrick, G.M. A short history of SHELX. *Acta Cryst.* **2008**, *64*, 112–122. [CrossRef] [PubMed]